Dynamic Contact Angles on Moving Plates

A simple model for advancing dynamic menisci of the interface between two immiscible fluids is proposed on the hypothesis that there is a monomolecular film which precedes an apparent contact line and that a frictional force due to the solid surface is balanced with the interfacial tension forces on the film. An analytical solution for dynamic contact angles on vertical and inclined solid surfaces of plates is obtained as a function of the interfacial capillary number, the static contact angle, and the parameters of Langumuir's duplex film model. An analytical solution for dynamic meniscus heights is also derived. The analytical solutions are compared with previous experimental data. The agreement between the theoretical and experimental results is found to be fairly good, average deviations being 3.8 and 12%, respectively, for dynamic contact angles and dynamic meniscus heights at the solid surface.

Kosaku Ishimi and Haruo Hikita
Department of Chemical Engineerng
University of Osaka Prefecture
Sakai, Osaka 591, Japan

M. N. Esmail
Department of Chemical Engineering
University of Saskatchewan
Sasekatoon, Sask. S7N 0W0, Canada

SCOPE

When analyzing the flow of a fluid as it moves over a solid surface and displaces another fluid, one encounters problems that have not yet been adequately resolved in the literature. One of the problems is a complete definition of the dynamic contact angle as a function of the relative velocity of the solid surface and the physical properties of the fluids. In spite of many experimental studies, the dynamic contact angles have not been related to the fluid viscosities or any specific physical properties of the fluids, especially at low relative velocity (Schwartz and Tejada, 1972; Kennedy and Burley, 1977). Another problem is encountered when one considers the flow near the contact line of the advancing interface between two fluids at the solid surface. Application of the classical no-slip boundary condition has led to the unbounded force at the contact line (Huh and Scriven, 1971).

Bascom et al. (1964) and Radigan et al. (1974) found extremely thin liquid films that preceded the moving apparent contact line during the spontaneous spreading of liquids on horizontal and vertical solid surfaces. On the basis of the assumption that this thin film is a monomolecular film which obeys the equation of state of the duplex film model by Langmuir (1933) and that a frictional force due to the solid surface is balanced with the interfacial tension forces on the film, analytical solutions for advancing dynamic contact angles and dynamic meniscus heights on vertical and inclined surfaces of plates moving in two immiscible fluids were derived and compared with the literature data.

CONCLUSIONS AND SIGNIFICANCE

Analytical solutions for advancing dynamic contact angles and dynamic meniscus heights on vertical and inclined surfaces of moving plates are obtained. The advancing dynamic contact angle is expressed as a function of the interfacial capillary number Ca_i ($=n\mu_i u_w RT/\sigma_{12}^2$), the static contact angle θ_s, and two dimensionless parameters of duplex film, A_i ($=A_0\sigma_{12}/RT$) and σ_i ($=\sigma_0/\sigma_{12}$). The analytical solutions are in fairly good agreement with the literature data available for dynamic contact angles θ and dynamic meniscus heights at the solid surface δ_w in gas-liquid-solid and liquid-liquid-solid systems, average deviations being 3.8 and 12% for θ and δ_w, respectively. This agreement gives strong support for the application of the proposed model to the prediction of dynamic wetting.

Correspondence concerning this paper should be addressed to Kosaku Ishimi.

Introduction

Dynamic contact angles are very important for meniscus shapes at the interface between two immiscible fluids and motions of the fluids relative to solid surfaces. They can be found in many different circumstances such as the spreading of adhesive, the flowing of lubricants into inaccessible locations, the displacement of oil by water through a porous medium, and the coating of solid surfaces with a thin, uniform layer of liquid.

Numerous experimental studies have been made of dynamic contact angles, and some experimental equations have been derived relating the dynamic contact angle to the relative velocity of the solid surface. In a low relative velocity field, however, the coefficients in these equations could not be related to any specific physical properties of the liquids and solid constituting the system (Schwartz and Tejada, 1972). On the other hand, many theoretical investigations have focused on the dynamics of the fluids surrounding the contact line and have encountered a discontinuity in velocity of the fluid at the contact line because of the conventional no-slip condition of fluid mechanics (Huh and Scriven, 1971; Dussan and Davis, 1974).

Since the dynamics of fluids surrounding the contact line is very complicated, a new approach will be required to understand the phenomena of dynamic menisci and to obtain a reasonable and practical equation for the dynamic contact angle. The present work was undertaken to present a simple model for advancing dynamic contact menisci for vertical and inclined surfaces of moving plates and to compare this model with previous experimental data.

Background

For the motion of a liquid slug in a cylindrical capillary tube filled with gas, it is well known that the driving pressure of the liquid is affected by the advancing and receding dynamic contact angles, the liquid surface tension, and the radius of the capillary, but is independent of the liquid viscosity when the liquid slug moves slowly (Birkerman, 1970). Another evidence of independence of viscosity can be found in an experimental study by Kennedy and Burley (1977) of dynamic menisci on a tape entering into a stationary liquid. They found that the dynamic meniscus can be considered as a quasi-static equilibrium profile and the effect of viscosity on the dynamic meniscus can be neglected for the case of low velocity of the tape. The independence of viscosity of advancing dynamic menisci indicates that the rate-controlling step is not the ordinary momentum transfer process near the solid surface and the meniscus of the interface.

Bascom et al. (1964) studied the spontaneous spreading of hydrocarbon liquids on the horizontal and vertical surfaces of the solid. They reported extremely thin films that preceded the moving apparent contact line observed macroscopically. Radigan et al. (1974) also detected thin films during the spreading of drops of glass on Fernico metal. The extremely thin films may be monomolecular layers and the existence of the thin film of liquid may be due to surface diffusional process over the solid surface (Bascom et al.) although the process is poorly understood. Therefore it seems that the advance of the thin film over the solid surface is a rate-determining factor. To our knowledge, no report has referred to thin films for the cases of advancing slugs in a capillary tube or plates plunging into a pool of liquid (Schwartz and Tejada, 1972). However, we can expect the existence of thin films for the cases described above, since the flow mechanism is analogous to that for the spontaneous spreading of liquids on solid surfaces.

Model

Consider a dynamic meniscus for a solid plate which, while moving in fluid 2 enters into a stationary fluid 1, at an angle of incidence of the plate α. Fluids 1 and 2 are immiscible. The situation is shown in Figure 1, where the solid and dotted lines represent the dynamic and static menisci, θ and θ_s are the advancing dynamic and static contact angles, and point C is the apparent contact line. Figure 2 shows the neighborhood of the apparent contact line C, where a stationary thin film of monomolecular layer of length ℓ is at the left side of the apparent contact line C and the solid surface moves toward the right at a constant velocity u_w.

Fluids 1 and 2 slip on the solid surface and are not affected by the motion of the solid surface because of the independence of viscosities of fluids on a dynamic meniscus, as described in the preceding section. Therefore fluids 1 and 2 are considered to be apparently stationary. On the other hand, the thin film also slips on the solid surface and is considered to be at rest. However it is influenced by a kind of frictional force due to the motion of the solid surface. If the frictional force per unit area τ_w is assumed to be proportional to the velocity of the solid surface u_w, τ_w can be given by

$$\tau_w = \mu_i u_w \tag{1}$$

where μ_i is a coefficient of friction.

As shown in Figure 2, on the other hand, the interfacial tension σ_{s2} between the solid and fluid 2 pulls the thin film toward the left. The interfacial tension σ_{s1} between the solid and fluid 1 and the horizontal component of the interfacial tension σ_{12} between fluid 1 and fluid 2 act toward the right. Since the advancing dynamic contact angle θ is larger than the static contact angle θ_s, the value of $\sigma_{s2} - (\sigma_{12} \cos\theta + \sigma_{s1})$ is positive. Therefore the interfacial pressure of the thin film σ—defined by the difference between the interfacial tension σ_{s2} between solid and fluid 2 and the interfacial tension of the thin film (Adamson, 1976)—acts toward the left and is balanced with the fric-

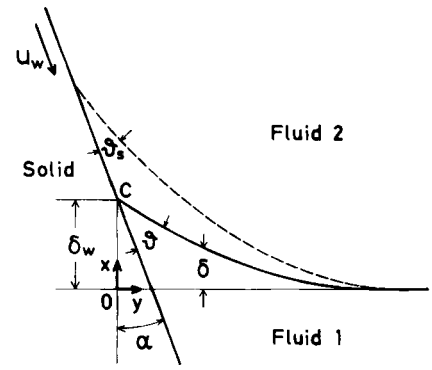

Figure 1. Dynamic meniscus over a moving solid surface and coordinate system.

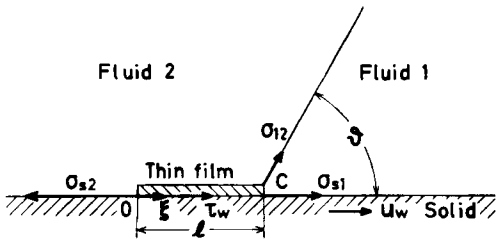

Figure 2. Definition of terms for flow perpendicular to contact line *C*.

tional force described above. Thus the force balance can be written as

$$d\sigma/d\xi = \tau_w \tag{2}$$

and the boundary conditions are expressed as

$$\xi = 0; \quad \sigma = 0 \tag{3}$$

$$\xi = \ell; \quad \sigma = \sigma_{s2} - \sigma_{12}\cos\theta - \sigma_{s1} \tag{4}$$

where ξ is the distance from the left edge of the thin film. Further, the interfacial pressure of the thin film σ is given by the equation of state of the thin film. Although several equations of state were proposed, in the present study it is simply assumed that the equation of state can be expressed as

$$(\sigma + \sigma_0)(A - A_0) = RT \tag{5}$$

Equation 5 is based on Langmuir's (1933) duplex film model, which was proposed for a liquid expanded film. In Eq. 5, A is the molecular area and σ_0 and A_0 are parameters of the duplex film model. For the case of $\sigma_0 = 0$ and $A_0 = 0$, the thin film is a perfect gaseous film. For the case of $\sigma_0 = 0$, the thin film corresponds to an imperfect gaseous film. If the total number of molecules in the thin film per unit perimeter is n, it is given by

$$n = \int_0^{\ell} (1/A)d\xi \tag{6}$$

As can be seen in Appendix A, Eqs. 1 to 6 yield the following equation for advancing dynamic contact angles

$$\Delta\cos\theta - (1/A_i)\ln\{[1 + A_i(\sigma_i + \Delta\cos\theta)]/(1 + A_i\sigma_i)\} = A_i Ca_i \tag{7}$$

where $\Delta\cos\theta$ is the difference between $\cos\theta_s$ and $\cos\theta$ given by

$$\Delta\cos\theta = \cos\theta_s - \cos\theta \tag{8}$$

Ca_i is the interfacial capillary number defined by

$$Ca_i = n\mu_i u_w RT/\sigma_{12}^2 \tag{9}$$

and A_i and σ_i are the dimensionless parameters defined by

$$A_i = A_0\sigma_{12}/RT \tag{10}$$

$$\sigma_i = \sigma_0/\sigma_{12} \tag{11}$$

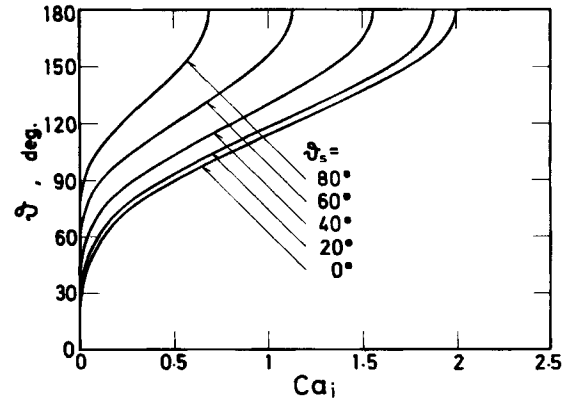

Figure 3. Dynamic contact angles for perfect gaseous film.

Figure 3 shows the dynamic contact angles θ for the case of perfect gaseous films. The values of dimensionless parameters A_i and σ_i for perfect gaseous films are equal to zero. In this case, Eq. 7 reduces to the following equation (Appendix A)

$$\Delta\cos\theta = \sqrt{2Ca_i} \tag{12}$$

Figure 4 represents the dynamic contact angle θ at θ_s equal to 60° for the case of imperfect gaseous films. In this case the dimensionless parameter σ_i is equal to zero. The value of $\Delta\cos\theta$

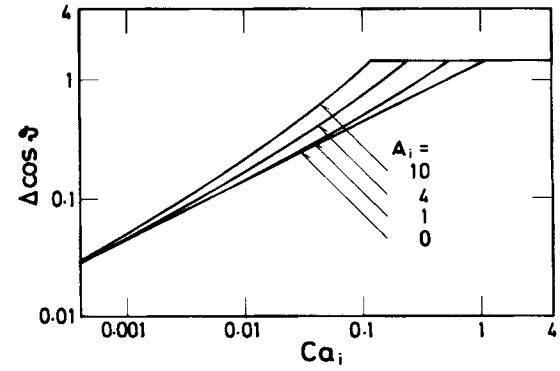

Figure 4. Dynamic contact angles for imperfect gaseous film at θ_s = 60°.

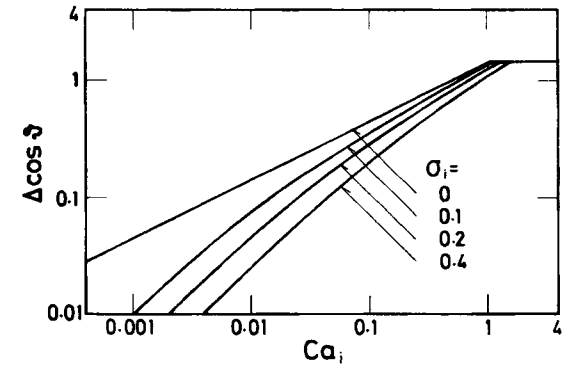

Figure 5. Dynamic contact angles for liquid expanded film at θ_s = 60° and A_i = 0.

increases with increasing Ca_i and A_i, and the effect of A_i on $\Delta \cos\theta$ becomes larger at higher values of Ca_i. Figure 5 shows the dynamic contact angles θ at $\theta_s = 60°$ and $A_i = 0$ for the case of a liquid expanded film. The value of $\Delta \cos\theta$ increases with increasing Ca_i and decreasing σ_i, but the effect of σ_i on θ becomes less pronounced at higher values of Ca_i.

Comparison with Experimental Data

Many experimental studies have been carried out on dynamic contact angles. However, few data are available because of the lack of some physical properties such as static contact angles. Perry (1967) studied dynamic contact angles on a magnetic tape entering vertically into a pool of ethanol. Kennedy and Burley (1977) measured dynamic contact angles on Mylar polyester tape plunging vertically into isopropanol. They also investigated the meniscus shapes of the interface between liquid and air. Gutoff and Kendrick (1982) measured the dynamic contact angles of various liquids on a gelatin-subbed polyester tape. They also studied the effect of the upper fluid on the dynamic contact angles by replacing air with immiscible oil.

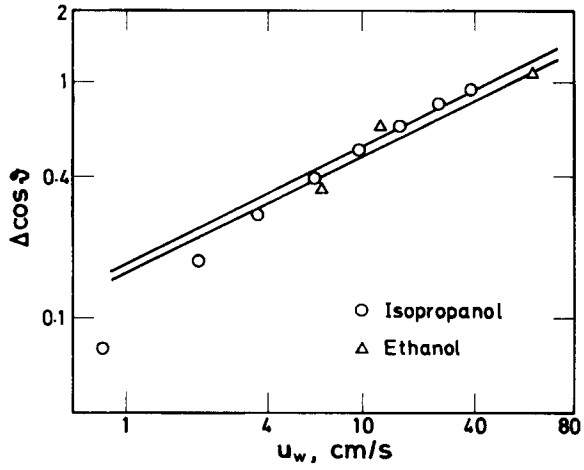

Figure 6. Comparison with experimental data in air-liquid-solid systems by Perry and by Kennedy and Burley.

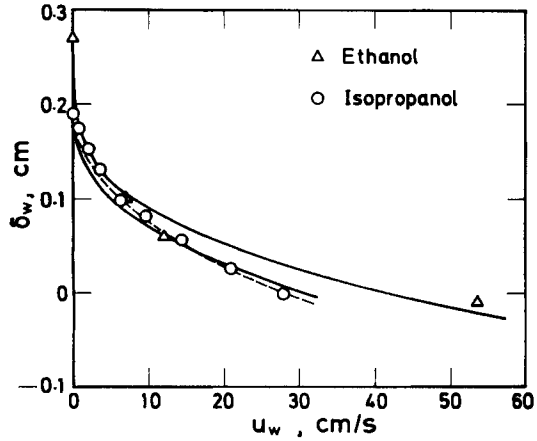

Figure 7. Comparison with experimental data in air-liquid-solid systems by Perry and by Kennedy and Burley.

Figures 6 and 7 respectively show the experimental data for the dynamic contact angle θ and the dynamic meniscus height δ_w at the solid surface obtained by Perry and by Kennedy and Burley. Figures 8 and 9 show the dynamic contact angles in air-liquid-solid systems obtained by Gutoff and Kendrick. Figure 11 represents the dynamic contact angles in immiscible oil-water-solid systems obtained by Gutoff and Kendrick.

To compare these experimental data with the theory presented in the preceding section, the values of the coefficient of friction μ_i, the total number of molecules of thin film n, and the

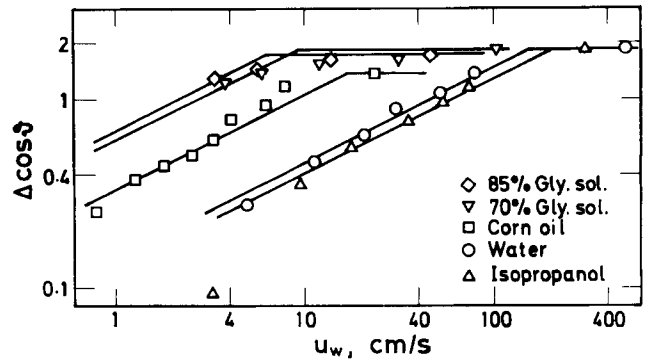

Figure 8. Comparison with experimental data in air-liquid-polyester systems by Gutoff and Kendrick.

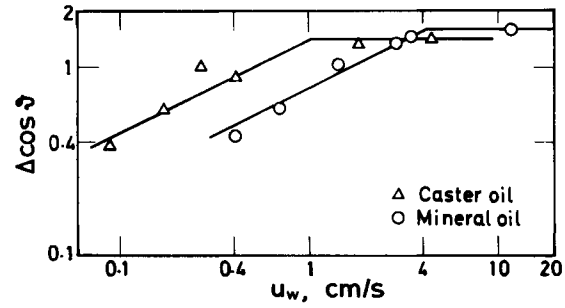

Figure 9. Comparison with experimental data in air-liquid-polyester systems by Gutoff and Kendrick.

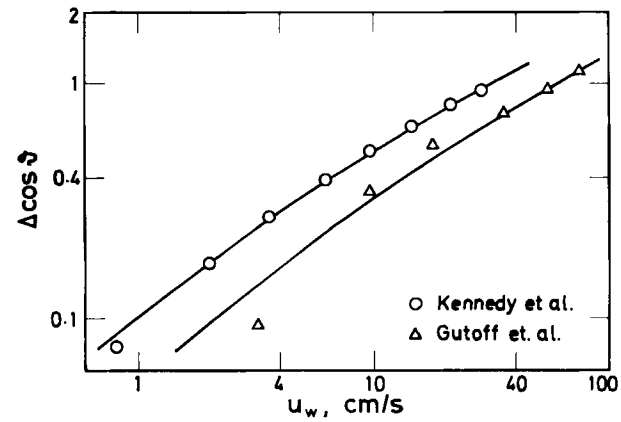

Figure 10. Comparison with experimental data in air-isopropanol-solid systems by Kennedy and Burley and by Gutoff and Kendrick.

Table 1. Fluid Properties in Air-Liquid-Solid Systems (Perfect Gaseous Film)

Fluid 1	Solid	ρ_l kg/m^3	$\sigma_{12} \times 10^3$ N/m	θ_s deg	$n\mu_i \times 10^7$ N · s · mol/m^4	Investigators
Ethanol	Magnetic tape	791	23	0	2.55	Perry
Isopropanol	Polyester	785	22	20.6	2.67	Kennedy and Burley
Water	Polyester	1,000	72	32	22.9	Gutoff and Kendrick
Isopropanol	Polyester	785	22	31	1.56	Gutoff and Kendrick
70% glycerol aq. sol.	Polyester	1,180	63	35	291.0	Gutoff and Kendrick
85% glycerol aq. sol.	Polyester	1,220	63	44	373.0	Gutoff and Kendrick
Corn oil	Polyester	923	34	68	27.2	Gutoff and Kendrick
Mineral oil	Polyester	880	32	53	128.0	Gutoff and Kendrick
Caster oil	Polyester	969	35	65	525.0	Gutoff and Kendrick

Table 2. Fluid Properties in Liquid-Water-Polyester System of Gutoff and Kendrick (Imperfect Gaseous Film)

Fluid 2	ρ_1 kg/m^3	ρ_2 kg/m^3	$\sigma_{12} \times 10^3$ N/m	θ_s deg	$n\mu_i \times 10^7$ N · s · mol/m^4	$A_0 \times 10^5$ m^2/mol
Kerosene	1,000	819	33	66	82.9	11.0
Corn oil	1,000	923	27	71	1,380	0.0
Mineral oil	1,000	880	55	68	108	76.8
Castor oil	1,000	969	26	74	711	8.41

parameters of the duplex film model σ_0 and A_0 should be given. However, there are no useful methods to estimate these values. In the present study these values are assumed to be constant in a system and to be independent of the velocity of solid surface u_w.

As can be seen in Figures 6, 8, and 9, the experimental values of $\Delta \cos \theta$ are approximately proportional to the square root of u_w except in isopropanol systems. This effect of u_w on $\Delta \cos \theta$ is similar to that in Eq. 12. In gas-liquid-solid systems, therefore, it is assumed that the thin films are perfect gaseous films and the values of A_0 and σ_0 are equal to zero. The values of $n\mu_i$ were determined by equating the value of a dynamic contact angle predicted from theory to a data point under a given experimental condition. The determined values of $n\mu_i$ are shown in Table 1. The solid lines in Figures 6, 8, and 9 show the theoretical equation for the dynamic contact angles, Eq. 7 with $A_i = 0$ and $\sigma_i = 0$. The solid lines in Figure 7 represent the theoretical equation for the dynamic meniscus height, Eq. B8, at the solid surface (Appendix B). As can be seen in these figures, the agreement between the experimental data and the theoretical predictions is fairly good except in isopropanol systems. In isopropanol systems, the experimental data of $\Delta \cos \theta$ lie considerably below the theoretical lines at the lower values of u_w. The difference between the experimental data and the predicted value may be due to the assumption of a perfect gaseous film. The effect of Ca_i on $\Delta \cos \theta$ in isopropanol systems seems to be the same as that for liquid expanded films in Figure 5. Therefore, the thin films are assumed to be liquid expanded films for $A_0 = 0$ in isopropanol systems. The values of $n\mu_i$ and σ_0 were determined by a method similar to that described above. The values of $n\mu_i$ and σ_0 are, respectively, 3.98×10^{-7} N·s·mol/m^4 and 3.25×10^{-3} N/m in the system of Kennedy and Burley, and 2.26×10^{-7} N·s·mol/m^4 and 4.10×10^{-3} N/m in the system of Gutoff and Kendrick. Figure 10 shows the comparison of the experimental data with the theoretical equation for dynamic contact angle, Eq. 7 with $A_i = 0$, for isopropanol systems. The broken line in Figure 7 represents the theoretical line for δ_w, Eq. B8, with Eq. 7 for $A_i = 0$. The agreement between the experimental data and the theoretical predictions is fairly good. In gas-liquid-solid systems, average deviations of the data points are 7.2 and 12% for $\Delta \cos \theta$ and δ_w, respectively.

In liquid-liquid-solid systems, the thin films are assumed to be imperfect gaseous films. The values of $n\mu_i$ and A_0 were determined by a similar method in gas-liquid-solid systems and are shown in Table 2. The solid lines in Figure 11 represent the theoretical equation for dynamic contact angles, Eq. 7 with $\sigma_i = 0$. The data points are in fairly good agreement with the theoretical lines, with an average deviation of 8.4%.

In both systems of gas-liquid-solid and liquid-liquid-solid, the dynamic contact angles can be predicted from Eq. 7 with an average deviation of 3.8%. The results indicate that the proposed model satisfactorily describes the dynamic wetting, although further experimental work in other systems, and studies of the coefficient of friction μ_i and the total number of molecules in thin film n, will be required to test the general applicability of the proposed model.

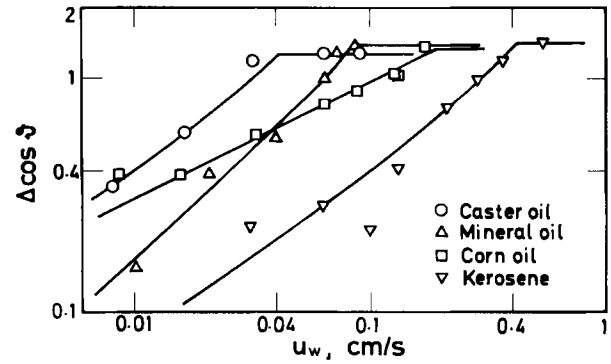

Figure 11. Comparison with experimental data in liquid-water-polyester systems by Gutoff and Kendrick.

Notation

A = molecular area, m^2/mol
A_i = dimensionless parameter, $A_0\sigma_{12}/RT$
A_0 = parameter of duplex film model, m^2/mol
Ca_i = interfacial capillary number, $n\mu_i u_w RT/\sigma_{12}^2$
g = acceleration due to gravity, m/s^2
ℓ = length of thin film, m
h = dimensionless meniscus height, Eq. B5
h_w = dimensionless meniscus height at solid surface, Eq. B6
n = total number of molecules in thin film per unit perimeter, mol/m
P_1, P_2 = static pressure of fluid 1 and fluid 2, Pa
P_∞ = static pressure at $y = \infty$, Pa
R = gas constant, $J/mol \cdot K$
T = absolute temperature, K
u_w = velocity of solid surface, m/s
x = vertical distance from horizontal interface
y = horizontal distance from apparent contact line

Greek letters

α = angle of incidence of plate, deg
$\Delta \cos\theta$ = difference between $\cos\theta_s$ and $\cos\theta$, Eq. 8
δ = dynamic meniscus height, m
δ_w = dynamic meniscus height at solid surface, m
θ = dynamic contact angle, deg
θ_s = static contact angle, deg
μ_i = coefficient of friction, kg/m^2s
ξ = distance from the left edge of thin film, m
ρ_1, ρ_2 = densities of fluid 1 and fluid 2, kg/m^3
σ = interfacial pressure of thin film, N/m
σ_c = interfacial pressure of thin film at apparent contact line, N/m
σ_i = dimensionless parameter, σ_0/σ_{12}
σ_{s1} = interfacial tension between solid-fluid 1, N/m
σ_{s2} = interfacial tension between solid-fluid 2, N/m
σ_{12} = interfacial tension between fluid 1-fluid 2, N/m
σ_0 = parameter of duplex film model, N/m
τ_w = frictional force per unit area, N/m^2

Appendix A: Derivation of Equation for Dynamic Contact Angles

Substituting Eq. 1 into Eq. 2 and solving the resulting equation under the boundary conditions of Eqs. 3 and 4, we obtain

$$\sigma = \mu_i u_w \xi \tag{A1}$$

$$\sigma\,|_{\xi=\ell} = \sigma_c = \sigma_{s2} - \sigma_{12}\cos\theta - \sigma_{s1} = \mu_i u_w \ell \tag{A2}$$

Substitution of Eqs. 5, A1, and A2 into Eq. 6 gives the following equation

$$\sigma_c - (RT/A_0)\ln\{[A_0(\sigma_c + \sigma_0) + RT]/[A_0\sigma_0 + RT]\} = n\mu_i A_0 u_w \tag{A3}$$

When the solid surface is stationary, on the other hand, the dynamic contact angle θ is equal to the static contact angle θ_s and Eq. A2 reduces to the well-known Young's equation.

$$\sigma_{s2} = \sigma_{12}\cos\theta_s + \sigma_{s1} \tag{A4}$$

The interfacial pressure σ_c at the apparent contact line is obtained from Eqs. A2 and A4, and is given by

$$\sigma_c = \sigma_{12}(\cos\theta_s - \cos\theta) \tag{A5}$$

Substituting Eq. A5 into Eq. A3 and rewriting the resulting equation with the dimensionless numbers $\Delta\cos\theta$, Ca_i, A_i, and σ_i, we can obtain the equation for dynamic contact angles, Eq. 7.

For the case of an imperfect gaseous film, the dimensionless parameter σ_i is equal to zero. In this case, Eq. 7 can be written

$$Ca_i = [A_i\Delta\cos\theta - \ln(1 + A_i\Delta\cos\theta)]/A_i^2 \tag{A6}$$

For the case of a perfect gaseous film, the dimensionless parameters A_i and σ_i are equal to zero. The righthand side of Eq. A6 is indeterminate at $A_i = 0$. However the limit can be evaluated by L'Hopital's rule, and Eq. A6 reduces to Eq. 12.

Appendix B: Dynamic Meniscus Height

Consider the dynamic meniscus as shown in Figure 1. As described in the section Model, the effect of viscosities on a dynamic meniscus can be neglected and the force balance for fluids 1 and 2 can be expressed as

$$dPj/dx = -\rho_j g \quad (j = 1, 2) \tag{B1}$$

The boundary conditions are given by

$$x = \delta,\ y > 0;\quad P_2 = P_1 + \sigma_{12}(d^2\delta/dy^2)/[1 + (d\delta/dy)^2]^{3/2} \tag{B2}$$

$$x = 0,\ y \to \infty;\quad P_1 = P_2 = P_\infty \tag{B3}$$

Solving Eq. B1 under Eqs. B2 and B3, we can obtain the following equation giving the meniscus height.

$$\sqrt{2 - h_w^2} - \sqrt{2 - h^2} + \frac{1}{\sqrt{2}}\ln\left[\frac{h_w(\sqrt{2} + \sqrt{2 - h^2})}{h(\sqrt{2} + \sqrt{2 - h_w^2})}\right] = \sqrt{\frac{(\rho_1 - \rho_2)g}{2\sigma_{12}}}\,y \tag{B4}$$

$$h = \delta\sqrt{(\rho_1 - \rho_2)g/2\sigma_{12}} \tag{B5}$$

$$h_w = \delta_w\sqrt{(\rho_1 - \rho_2)g/2\sigma_{12}} \tag{B6}$$

On the other hand, the gradient of the meniscus height at the solid surface is given by

$$d\delta/dy|_{y=0} = -\tan(\pi/2 - \theta - \alpha) \tag{B7}$$

Substitution of Eq. B4 into Eq. B7 gives the dimensionless meniscus height h_w at the solid surface, which can be written as

$$h_w^2 = 1 - \sin(\theta + \alpha) \tag{B8}$$

The dynamic contact angle θ can be obtained from Eq. 7, and therefore the dynamic meniscus height can be calculated from Eqs. 7, B4, and B8.

Literature Cited

Adamson, A. W., *Physical Chemistry of Surfaces*, 3rd ed., Wiley, New York, 81 (1976).

Bascom, W. D., R. L. Cottington, and C. R. Singleterry, "Dynamic Surface Phenomena in the Spontaneous Spreading of Oils on Solids" in *Contact Angles, Wettability and Adhesion*, Am. Chem. Soc., Washington, DC, 355–379 (1964).

Birkerman, J. J., *Physical Surface,* Academic Press, New York, 276 (1970).
Dussan, V., E. B. and S. H . Davis, "On the Motion of a Fluid-Fluid Interface Along a Solid Surface," *J. Fluid Mech.*, **65,** 71 (1974).
Gutoff, E. B., and C. E. Kendrick, "Dynamic Contact Angles," *AIChE J.*, **28,** 459 (1982).
Huh, C., and L. E. Scriven, "Hydrodynamic Model of Steady Movement of a Solid Liquid/Fluid Contact Line," *J. Colloid Interface Sci.*, **35,** 85 (1971).
Langmuir, I., "Oil Lenses on Water and the Nature of Monomolecular Expanded Films," *J. Chem. Phys.*, **1,** 756 (1933).
Kennedy, B. S., and R. Burley, "Dynamic Fluid Interface Displacement and Prediction of Air Entraiment," *J. Colloid Interface Sci.*, **62,** 48 (1977).
Perry, R. T., "Fluid Mechanics of Entraiment through Liquid-Liquid and Liquid-Solid Junctions," Ph.D. Thesis, Chem. Eng., Univ. Michigan, 1966; University Microfilms, Ann Arbor, MI, 76-14, 639 (1967).
Radigan, W., et al., "Kinetics of Spreading of Glass on Fernico Metal," *J. Colloid Interface Sci.*, **49,** 241 (1974).
Schwartz, A. M., and S. B. Tejada, "Studies of Dynamic Contact Angles on Solids," *J. Colloid Interface Sci.*, **38,** 359 (1972).

Manuscript received Jan. 28, 1985, and revision received May 17, 1985.